# Establishment of Uncertainty Ranges and Probability Distributions of Actinide Solubilities for Performance Assessment in the Waste Isolation Pilot Plant

Yongliang Xiong[1], Jim Nowak[1*], Laurence H. Brush[1], Ahmed E. Ismail[1] and Jennifer Long[1]
[1]Sandia National Laboratories (SNL), 4100 National Parks Highway,
Carlsbad, NM 88220, U.S.A.

## ABSTRACT

The Fracture-Matrix Transport (FMT) code developed at Sandia National Laboratories solves chemical equilibrium problems using the Pitzer activity coefficient model with a database containing actinide species. The code is capable of predicting actinide solubilities at 25 $^{o}$C in various ionic-strength solutions from dilute groundwaters to high-ionic-strength brines. The code uses oxidation state analogies, i.e., Am(III) is used to predict solubilities of actinides in the +III oxidation state; Th(IV) is used to predict solubilities of actinides in the +IV state; Np(V) is utilized to predict solubilities of actinides in the +V state. This code has been qualified for predicting actinide solubilities for the Waste Isolation Pilot Plant (WIPP) Compliance Certification Application in 1996, and Compliance Re-Certification Applications in 2004 and 2009.

We have established revised actinide-solubility uncertainty ranges and probability distributions for Performance Assessment (PA) by comparing actinide solubilities predicted by FMT with solubility data in various solutions from the open literature. The literature data used in this study include solubilities in simple solutions (NaCl, $NaHCO_3$, $Na_2CO_3$, $NaClO_4$, KCl, $K_2CO_3$, etc.), binary mixing solutions (NaCl+$NaHCO_3$, NaCl+$Na_2CO_3$, KCl+$K_2CO_3$, etc.), ternary mixing solutions (NaCl+$Na_2CO_3$+KCl, $NaHCO_3$+$Na_2CO_3$+$NaClO_4$, etc.), and multi-component synthetic brines relevant to the WIPP.

## INTRODUCTION

Prediction of actinide solubilities with a reliable thermodynamic model is important to the performance assessment (PA) for geological repositories for nuclear waste. There are three activity coefficient models commonly employed in geochemical computer codes, i.e., the Davies equation, the B dot equation, and the Pitzer equation. The Davies equation is applicable only to very dilute solutions such as groundwater with ionic strength up to 0.1 m. The B dot equation is applicable to solutions with ionic strength up to 1.0 m. In contrast, the Pitzer equation is applicable to solutions with very high ionic strengths. The Fracture-Matrix Transport (FMT) code developed at Sandia National Laboratories employs the Pitzer activity coefficient model to solve chemical equilibrium problems including those involving actinide species [1-6].

The Waste Isolation Pilot Plant (WIPP) is a U.S. Department of Energy geological repository for the permanent disposal of defense-related transuranic (TRU) waste [7-8]. This geological repository is located 42 km east of Carlsbad in southeastern New Mexico. The repository is 655 m below the surface, and is situated in the Salado Formation, a Permian salt bed composed mainly of halite, and lesser amounts of anhydrite, gypsum, polyhalite, magnesite, clays and quartz. The Salado Formation is approximately 600 m thick [9]. The Rustler Formation is immediately above the Salado Formation. It is 95 m thick at the WIPP and consists

[*] Deceased.

of anhydrite, halite, siltstone, sandstone, and dolomite. The Castile Formation underlies the Salado, and is approximately 385 m thick at the WIPP [9]. It has three thick anhydrite units separated by halite layers [9]. There are brine reservoirs located in areas of structural deformation within the Castile [10]. The in situ temperature at a depth of 655 m (the repository horizon) is 28 $^{o}$C, which is also the expected temperature after the repository is filled and sealed because the TRU waste to be emplaced in the WIPP will not produce enough heat to increase the temperature significantly. The brines associated with the Salado and Castile Formations are of high ionic strengths (up to 8.26 m) in nature [11].

In the PA calculations, the baseline solubilities of actinide predicted by the FMT code are combined with sampled uncertainty factors describing possible deviations of the thermodynamic model from the expected behavior. The reason for employing uncertainty factors is to adjust the baseline solubilities up if the model underpredicts the experimentally measured solubilities, or to adjust the baseline solubilities down if the model overpredicts the measured solubilities. In this paper, we describe uncertainty ranges and probability distributions of actinide solubilities established for PA in the WIPP.

## THERMODYNAMIC MODEL

The FMT code uses oxidation state analogies, i.e., Am(III) being used to predict solubilities of actinide in the +III oxidation state; Th(IV) being employed to predict solubilities of actinide in the +IV state, and Np(V) being utilized to predict solubilities of actinide in the +V state. The following descriptions focus on Am(III) and Th(IV) models, as the WIPP PA does not sample the uncertainties in the solubility of Np(V) in view of the fact that releases of this element do not affect the long-term performance of the WIPP.

### Am(III) and Th(IV) models

In Table I, the aqueous species of Am(III) and Th(IV) models incorporated into the database of the FMT code are listed. The aqueous thermodynamic model of Am(III) includes $Am^{3+}$, americium carbonate complexes, chloride complexes, hydroxyl complexes, organic ligand complexes, and sulfate complexes. The aqueous thermodynamic model of Th(IV) includes $Th^{4+}$, thorium carbonate complex, hydroxyl complex, mixed carbonate and hydroxyl complex, organic ligand complexes, and sulfate complexes. The Pitzer interaction parameters of these Am(III) and Th(IV) species with major ions are listed in Table II. The sources of these thermodynamic parameters are detailed in [1] and [4].

**Table I**. Aqueous species and their Gibbs free energy of formation at reference state (298.15 K and 1 bar) of Am(III) model in the FMT code

| Species | $\Delta_f G$, kJ mol$^{-1}$ |
|---|---|
| $Am^{3+}$ | -599.116 |
| $AmCO_3^{+}$ | -1,173.200 |
| $Am(CO_3)_2^{-}$ | -1,729.026 |
| $Am(CO_3)_3^{3-}$ | -2,269.433 |
| $Am(CO_3)_4^{5-}$ | -2,784.705 |
| $AmOH^{2+}$ | -793.123 |

| | |
|---|---|
| $Am(OH)_2^+$ | -983.819 |
| $Am(OH)_3^o$ | -1,163.880 |
| $AmCl^{2+}$ | -731.747 |
| $AmCl_2^+$ | -857.424 |
| $AmSO_4^+$ | -2,109.450 |
| $Am(SO_4)_2^-$ | -1,362.260 |
| $AmAc^{2+}$ | -980.016 |
| $AmCit^o$ | -566.517 |
| $AmEDTA^-$ | -575.889 |
| $AmOx^+$ | -601.989 |
| $Th^{4+}$ | -704.547 |
| $Th(CO_3)_5^{-6}$ | -3,498.551 |
| $Th(OH)_3(CO_3)^-$ | -1,922.639 |
| $Th(OH)_4^o$ | -1,553.192 |
| $Th(SO_4)_2^o$ | -2,259.915 |
| $Th(SO_4)_3^{2-}$ | -3,009.286 |
| $ThAc^{3+}$ | -1,111.812 |
| $ThCit^+$ | -708.689 |
| $ThEDTA^o$ | -707.502 |
| $ThOx^{2+}$ | -737.270 |

Ac: Acetate; Cit: Citrate; Ox: Oxalate

$\Delta_f G$ are converted from $\mu^o/RT$ using $\Delta_f G = (\mu^o/RT) \times 298.15 \times 8.314$

**Table II**. Pitzer interaction parameters involving Am(III) and Th(IV) species

| Species *i* | Species *j* | $\beta^{(0)}$ | $\beta^{(1)}$ | $C^\phi$ |
|---|---|---|---|---|
| $Am^{3+}$ | $Cl^-$ | 0.5856 | 5.6 | -0.0166 |
| $Am^{3+}$ | $SO_4^{2-}$ | 1.792 | 15.04 | 0.600 |
| $AmCO_3^+$ | $Cl^-$ | -0.072 | 0.403 | 0.0388 |
| $AmOH^{2+}$ | $Cl^-$ | -0.055 | 1.6 | 0.05 |
| $Am(OH)_2^+$ | $Cl^-$ | -0.616 | -0.45 | 0.05 |
| $AmCl^{2+}$ | $Cl^-$ | 0.593 | 3.15 | -0.006 |
| $AmCl_2^+$ | $Cl^-$ | 0.516 | 1.75 | 0.010 |
| $AmSO_4^+$ | $Cl^-$ | -0.091 | -0.39 | 0.048 |
| $AmAc^{2+}$ | $Cl^-$ | 0.3088 | 1.74 | -0.132 |
| $AmOx^+$ | $Cl^-$ | -0.9374 | 0.29 | 0.248 |
| $Na^+$ | $Am(CO_3)_2^-$ | -0.240 | 0.224 | 0.0284 |
| $Na^+$ | $Am(CO_3)_3^{3-}$ | 0.125 | 4.73 | 0.0007 |
| $Na^+$ | $Am(CO_3)_4^{5-}$ | 2.022 | 19.22 | -0.305 |
| $Na^+$ | $Am(SO_4)_2^-$ | -0.345 | 0.40 | 0.051 |
| $Na^+$ | $AmEDTA^-$ | -0.2239 | 0.29 | 0.095 |
| Interaction parameters for neutral species and mixing parameters | | | | |
| Species *i* | Species *j* | $\lambda_{ij}$ | $\theta_{ij}$ | |
| $Am(OH)_3^o$ | $Na^+$ | -0.2 | | |
| $Am(OH)_3^o$ | $Cl^-$ | -0.2 | | |

| | | | | |
|---|---|---|---|---|
| $AmCit^{o}$ | $Cl^{-}$ | -0.406 | | |
| $Am^{3+}$ | $Ca^{2+}$ | | 0.2 | |
| $AmCl^{2+}$ | $Ca^{2+}$ | | -0.014 | |
| $AmCl_2^{+}$ | $Ca^{2+}$ | | -0.196 | |
| $Am^{3+}$ | $Na^{+}$ | | 0.1 | |
| Binary interaction parameters for Th(IV) species | | | | |
| $Th^{4+}$ | $Cl^{-}$ | 1.092 | 13.7; $\beta^{(2)}$= -160 | -0.112 |
| $Th^{4+}$ | $SO_4^{2-}$ | 1.56 | 0 | 0 |
| $Th^{4+}$ | $HSO_4^{-}$ | 1.44 | 0 | 0 |
| $ThAc^{3+}$ | $Cl^{-}$ | 1.061 | 5.22 | 0.109 |
| $ThCit^{+}$ | $Cl^{-}$ | -0.7467 | 0.29 | 0.319 |
| $ThOx^{2+}$ | $Cl^{-}$ | -0.343 | 1.74 | 0.5 |
| $Na^{+}$ | $Th(CO_3)_5^{-6}$ | 1.31 | 30 | 0 |
| $Na^{+}$ | $Th(SO_4)_3^{2-}$ | 0.12 | 0 | 0 |
| $K^{+}$ | $Th(SO_4)_3^{2-}$ | 0.90 | 0 | 0 |
| Interaction parameters for neutral species and mixing parameters | | | | |
| Species *i* | Species *j* | Species *k* | $\lambda_{ij}$ or $\theta_{ij}$ | $\Psi_{ijk}$ |
| $Th(SO_4)_2^{o}$ | $Cl^{-}$ | | 0.29 | |
| $Th(SO_4)_2^{o}$ | $HSO_4^{-}$ | | 0.68 | |
| $ThEDTA^{o}$ | $Cl^{-}$ | | 0.1111 | |
| $Th^{4+}$ | $Na^{+}$ | $Cl^{-}$ | 0.42 | 0.21 |
| $Th^{4+}$ | $Mg^{2+}$ | $Cl^{-}$ | 0.60 | 0.21 |
| $Th^{4+}$ | $H^{+}$ | $Cl^{-}$ | 0.60 | 0.37 |
| $Na^{+}$ | $Th(CO_3)_5^{-6}$ | $Cl^{-}$ | 2.0 | -0.08 |

## Establishment of Uncertainty Ranges and Probability Distribution of Actinide Solubilities

The uncertainty ranges and probability distribution of actinide solubilities are established by comparisons of predicted values with experimentally determined values under identical conditions. Experimental values used for derivation of thermodynamic parameters in the thermodynamic model are excluded from comparisons. Experimental solubility data are from a wide range of supporting electrolytes with various ionic strengths. Supporting solutions include simple solutions (NaCl, $NaHCO_3$, $Na_2CO_3$, $NaClO_4$, KCl, $K_2CO_3$, etc.), binary mixing solutions (NaCl+$NaHCO_3$, NaCl+$Na_2CO_3$, KCl+$K_2CO_3$, etc.), ternary mixing solutions (NaCl+$Na_2CO_3$+KCl, $NaHCO_3$+$Na_2CO_3$+$NaClO_4$, etc.), and multi-component synthetic brines relevant to the WIPP.

## RESULTS

Based on comparisons as mentioned above, probability distributions of Am(III) and Th(IV) models are presented in Figures 1 and 2. The *D* value, i.e., difference between measured values and experimentally determined values, is defined as:

$$D = \log_{10} S_m - \log_{10} S_p$$

where $S_m$ is experimental solubility data, and $S_p$ is predicted solubility.

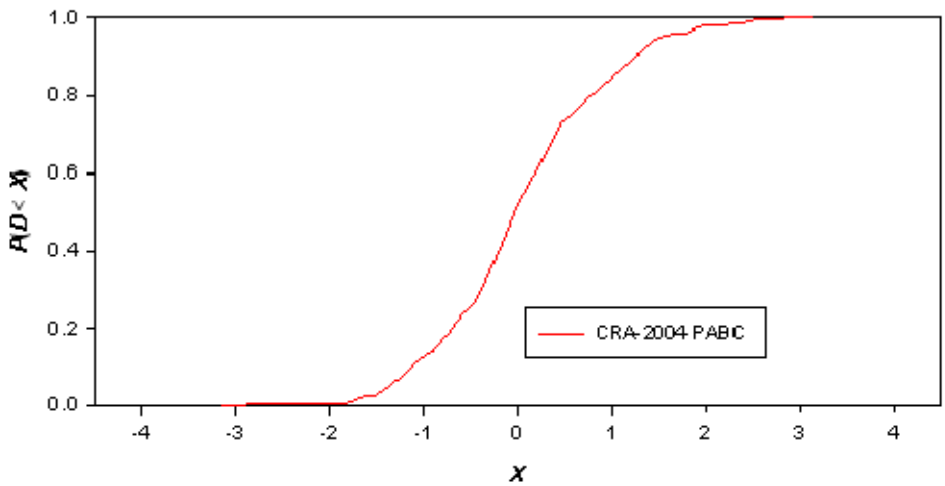


**Figure 1**. Cumulative distribution functions of Am(III) model for the Compliance Recertification Application 2004 Performance Assessment Baseline Calculations (CRA-2004 PABC).

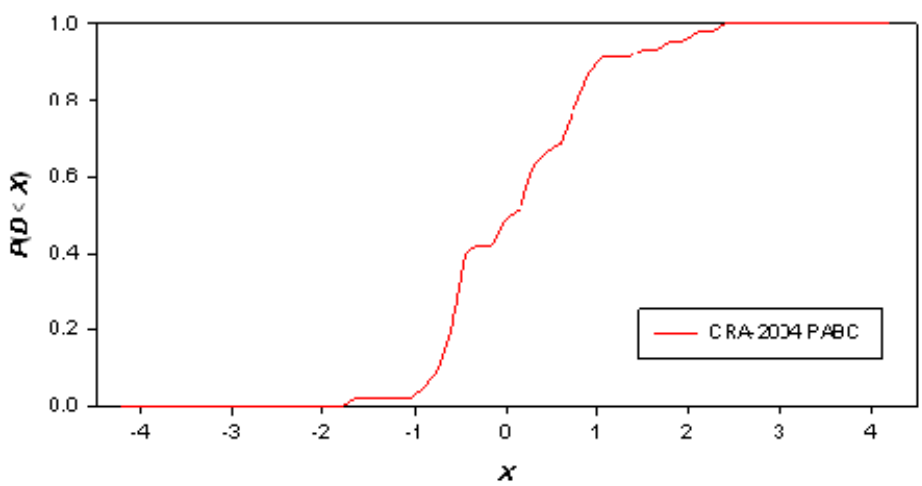


**Figure 2**. Cumulative distribution functions of Th(VI) model for the Compliance Recertification Application 2004 Performance Assessment Baseline Calculations (CRA-2004 PABC).

## CONCLUSIONS

The FMT code with the Pitzer activity coefficient model can predict actinide solubilities in brines with high ionic strengths at 25 $^{o}$C, and this code has been qualified for predicting actinide solubilities for the WIPP. Such predictions have been accepted by US EPA for the Compliance Certification Application and Re-Applications for the WIPP. In this paper, the

uncertainty ranges and probability distributions of actinide solubilities that were established by comparing measured experimental data with predicted values are presented.

## ACKNOWLEDGMENTS

This research is funded by WIPP programs administered by the U.S. Department of Energy. Sandia is a multiprogram laboratory operated by Sandia Corporation, a Lockheed Martin Company, for the United States Department of Energy's National Nuclear Security Administration under contract DE-AC04-94AL85000.

## REFERENCES

1. S.C. Babb and C.F. Novak, "User's Manual for FMT Version 2.3: A Computer Code Employing the Pitzer Activity Coefficient Formalism for Calculating Thermodynamic Equilibrium in Geochemical Systems to High Electrolyte Concentrations." Albuquerque, NM: Sandia National Laboratories, 1997.
2. E. Giambalvo, L.H. Brush and Y.-L. Xiong Y.-L, Eos Trans. AGU **83** (47), U11B-02 (2002).
3. C.F. Novak, J. Contaminant Hydrology 21, 297 (1996).
4. Y.-F. Wang, "WIPP PA Validation Document for FMT (Version 2.4), Document Version 2.4." Carlsbad, NM: Sandia National Laboratories, 1998.
5. Y.-L. Xiong, "Release of FMT_050405.CHEMDAT." Carlsbad, NM: Sandia National Laboratories, ERMS 539304, 2005.
6. Y.-L. Xiong, E.J. Nowak and L.H. Brush, Geochimica et Cosmochimica Acta **69**(10), Supp.1, A417, (2005).
7. U.S. DOE, "Title 40 CFR Part 191 Compliance Certification Application." DOE/CAO 1996-2184. Carlsbad, NM: U.S. DOE Carlsbad Area Office, 1996.
8. U.S. DOE, "Title 40 CFR Part 191 Compliance Recertification Application for the Waste Isolation Pilot Plant, Vol. 1-8." DOE/WIPP 2004-3231. Carlsbad, NM: U.S. DOE Carlsbad Field Office, 2004.
9. D.W. Powers, S.J. Lambert, S.-E. Shaffer, L.R. Hill, W.D. Weart, Eds., "Geological Characterization Report, Waste Isolation Pilot Plant (WIPP) Site, Southeastern New Mexico, Vols. I and II." SAND 78-1596. Albuquerque, NM: Sandia National Laboratories, 1976.
10. R.S. Popielak, R.L. Beauheim, S.R. Black, W.E. Coons, C.T. Ellingson and R.L. Olsen, "Brine Reservoirs in the Castile Formation, Waste Isolation Pilot Plant Project, Southeastern New Mexico." TME 3153. Carlsbad, NM: U.S. DOE WIPP Project Office, 1983.
11. Y.-L. Xiong and A.S. Lord, Applied Geochemistry 23, 1634 (2008).